Volume 4, No. 5, May 2013

Journal of Global Research in Computer Science

ISSN-2229-371X

RESEARCH PAPER

Available Online at www.jgrcs.info

NEW REGION GROWING ALGORITHM FOR BRAIN IMAGES SEGMENTATION

Sultan Aljahdali[†], E. A. Zanaty[†‡], Ashraf Afifi[†]

[†]Computer Science Dept., College of Computers and IT, Taif University, Taif, Saudi Arabia.

[‡]Computer Dept., College of Science, Sohag University, Sohag, Egypt.

Abstract: Segmentation of medical images is challenging due to the poor image contrast and artifacts that result in missing tissue boundaries, i.e. pixels inside the region have similar intensity. In this paper, we introduce a new automatic method for region growing capable to segment 2D/3D Magnetic Resonance Images (MRI) and Computed Tomography (CT) which contain weak boundaries between different tissues. The proposed method is used to extract reliable regions of an image to produce a computer aided design for 3D images. It includes an automatic threshold and is based on estimating probability of pixel intensities of a given image. An automatic threshold is computed as a function of intensity and probability of pixels. This makes the threshold to be flexible and can give large threshold when pixels have very similar intensities and small when they are on the boundaries. The experimental results show that the proposed technique produces accurate and stable results.

Keywords*:* Medical imaging segmentation, region growing, automatic threshold, MRI, CT, weak boundaries.

INTRODUCTION

Medical imaging includes conventional projection radiography, Computed Tomography (CT), Magnetic Resonance Images (MRI) and ultrasound, MRI and CT images provide 3D data. However, the amount of data is far too much for manual analysis/ interpretation, and this has been one of the biggest obstacles in the effective use of MRIs. Medical image segmentation algorithms often face difficult challenges such as poor image contrast, noise, and missing or diffuse boundaries.

The segmentation of region is an important first step for variety image related application and visualization tasks. Also, segmentation of medical images is important since it provides assistance for medical doctors to find out the diseases inside the body without the surgery procedure, to reduce the image reading time, to find the location of a lesion and to determine an estimate of the probability of a disease.

Segmentation of brain MRIs into different tissue classes, especially Gray Matter (GM), White Matter (WM), is an important task. Brain MRIs have low contrast between some different tissues. In many images, the problem of MRIs is the low contrast between tissues. Therefore, previous works [1,2,11,13,14,16-22] extracted these tissues as one tissue.

Brain MRIs with weak boundaries have very similar pixels value around the boundaries so it is difficult to segment this tissue by previous works. Region Growing (RG) method can not specify the tissues segmentation with weak boundaries because the growing of the region will not stop on the boundaries and will add outside pixels of the tissue to the organ.

To solve this problem, we present an automatic RG technique capable to segment tissues with weak boundaries. The proposed RG method includes a threshold that can be varied over the image and is computed as a function of probability of image intensity to improve the regions cuts. The probability of image pixels is used here to force the growing region to stop to add pixels from the other tissues to the region, i.e. the threshold is used when pixels have very similar intensities and small when they are on the boundaries. The proposed method is applied to MRIs and CT images to prove its efficiency. The tested MRIs and CT images contain background and object with one or more tissues with weak boundaries.

The rest of the paper is organized as follows. The related works is discussed in section 2. Section 3 presents RG technique. The proposed method is described in section 4. The results obtained with both simulated brain and CT data are presented in Section 5. Our conclusion is presented in section 6.

RELATED WORKS

There are many types of image segmentation techniques [1-23], among them: histogram-based [6,10] and region-based [4,19-23] techniques are most popular. Many researchers have tried to solve threshold problem in histogram- and region-based [1-23]. However, it is really difficult to find a general threshold for all cases to determine the threshold value for segmentation.

The histogram-based segmentation technique produces a binary image based on the threshold value. The intensities of object and background pixels tend to cluster into two sets in the histogram with threshold between these two sets. The histogram-based technique only considers the histogram of the image without checking the spatial relationship among connected pixels.

The region-based segmentation technique segments an image which has strong boundaries into several small regions, followed by merge procedure using specific threshold. In both segmentation techniques, if the threshold is not appropriate, the contour of object will be destroyed. Ayman et al. [3] presented RG technique for medical image segmentation and obtained a good results for low noise level but for high noise level the results was the same as in Del-Fresno et al.[4]. Wu et al. [6] presented a top down region-based image segmentation technique for medical images contain three major regions: background and two tissues. This method can only segment 2D images and cannot segment 3D images or images which contain more than two tissues. The technique in [12] handles image segmentation using only region-based image features with the assumption that only object and background exist in the image.

Graph cut image segmentation techniques [8,13,16] used two kinds of seed pixel as "object" and "background", to provide hard constraints for segmentation. In these techniques, we need to put seeds pixel in each tissue which describe as background, and these techniques describe each pixel in the image to belong to object or belong to background.

Forouzanfar et al. [1] presented a study investigating the potential of genetic algorithms and particle swarm optimization to determine the optimum value of degree of attraction. This technique can only segment 2D MRIs which have a known number of tissues. Baillard et al. [15] used level set approach to segment brain 3D MRIs but this level set technique extracted brain from MRIs and can not extract WM or GM from the same images.

REGION GROWING TECHNIQUE

RG is an approach to image segmentation in which neighboring pixels are examined and added to a region class. This technique used only a few seed pixels as "object", and described each pixel in the object to belong to the object or belong to the edges of this object. RG [19-23] have the threshold problem and can not segment images contain weak boundaries.

The simple RG technique consists in merging neighboring pixels P_x of the pixel P_y, inside the region, according to $|I(P_x) - I(P_y)| \leq T$, where T is a fixed threshold and $I(\bullet)$ is the pixel intensity value. This technique has two problems, 1) the choice of the threshold and 2) this technique can lead to a chaining effect especially for image with pixel intensity changing gradually. The second problem can be solved by using the homogeneity test $f(I_{i,j})=| I_{i,j} - RA| \leq T$, where RA is the region average (the summation of pixels intensities over the number of pixels inside the region).

This technique used different fixed threshold for each tissue in the image. The fixed threshold cross the function $f(I_{i,j})$ in two points ($a < RA$ and $b > RA$ see Figure 1) with the same distant from RA, if T which is a linear function is not correct and small then pixels inside the tissue will be described as outside, and if it big some pixels outside the tissue will be added to the region specially when the tissue has weak boundaries.

RG technique iteratively merge similar pixels into sets or merge sub-regions into larger regions in 3 main steps: (1) choice of the seed pixels; (2) neighborhood analysis according to a similarity rule, and (3) grow the seed regions by including adjacent pixels that satisfy the similarity rule. The steps (1) and (2) are repeated until there are no more adjacent pixels to be included in a seed region. In the next section, we will solve the choice of threshold problem.

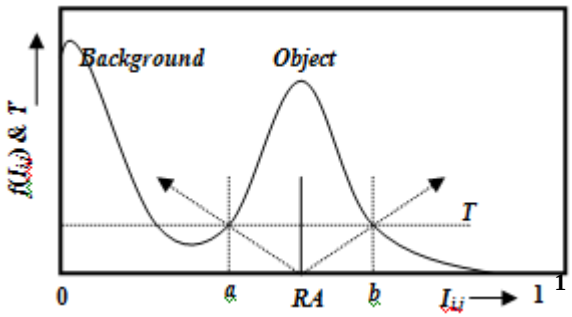

Figure 1. The function $f(I_{i,j})$ with fixed threshold

THE PROPOSED TECHNIQUE

Weak Boundary:

In MRIs, intensity non-uniformity can affect computational analysis of the image due to the variance in signal intensity. It is manifested as smooth spatially varying signal intensity across the image and caused by several factors including inhomogeneous radiofrequency (RF) fields (caused by distortion of the RF field by the object being scanned or non-uniformity of the transmission field). The boundaries among tissues become weak when RF and noise increase.

Furthermore, inside each tissue the pixels of the region have very similar intensities and outside each tissue the pixels have different intensities from inside the region. Also, the pixels on the boundaries will have intensities between the intensities inside and outside. The boundaries become strong if there is big difference between the pixels inside and outside the tissues, and become weak if the difference is small.

In both cases, the pixels intensities on the boundaries have different values from inside and outside pixels intensities. Furthermore, the numbers of pixels which have the same intensity inside or outside the tissue(s) are much bigger than the number of pixels on the boundaries. So, probabilities of these pixels intensities in the tissue or in the other tissues have higher value than pixels intensities on the boundaries.

The histogram-based technique used only the number of pixels with the same intensities for segmentation. The region-based technique used the connectivity between pixels without using the number of pixels with the same intensities in the

image. Our idea is to use probabilities (which related to pixels number) to give large threshold for RG when pixels have similar intensities and small when they are on the boundaries.

An Automatic Threshold:

In this section, we discuss in more details about the proposed method. We present an automatic threshold method to identify the pixels that have similar intensities. We will use pixel intensity and probability of pixel intensity in RG technique to extract only the tissue(s) which the user will choose. The threshold will be calculated for each pixel inside the region by using pixel intensity value $I_{i,j}$ and probability of pixel intensity $\Pr(I_{i,j})$.

We define threshold function T as a nonlinear function, this function will cut and cross $f(I_{i,j})$ at least in one pixel intensity. T will cut $f(I_{i,j})$ in backward pixel intensity ($I_{i,j} < RA$) and in forward pixel intensity ($I_{i,j} > RA$) when we extracted bright and very dark tissues respectively. We suppose that

$$f(I_{i,j}) = \left| I_{i,j} - RA \right| \le T\left(I_{i,j}, \Pr(I_{i,j})\right). \qquad (1)$$

Since the boundaries become weaker when RF and noise levels increasing, so threshold value should be smaller on boundaries pixels than threshold in non-boundaries pixels. To extract a tissue with weak boundaries, the region will be stopped growing in the first pixel outside the tissue(s). We define the threshold function as follows:

$$T\left(\Pr(I_{i,j}), I_{i,j}\right) = T_1(I_{i,j})\, T_2\left(\Pr(I_{i,j})\right); \quad 0 \le I_{i,j} \le 1, \qquad (2)$$

where

$$T_1(I_{i,j}) = \begin{cases} I_{i,j}^{2\gamma} & I_{i,j} < \theta, \\ (1 - I_{i,j})^{2\alpha} & I_{i,j} > \theta, \end{cases} \qquad (3)$$

$$T_2\left(\Pr(I_{i,j})\right) = e^{\beta}, \quad \beta = -\beta_1 \left| \log\left(\Pr(I_{i,j})\right) \right|^{-1}. \qquad (4)$$

and θ occur outside the choosing tissue(s).

We used different MRIs to calculate β_1 and found that $\alpha = \gamma$ takes very small value in very dark tissue and this value increases when we extract dark tissue, and increases more when we extract bright tissue. So, we put $\beta_1 = I_{i,j}^{1/2}$ where $\beta_1 \in [0,1]$. In the same way, we put $\beta_1 = (1 - I_{i,j})^{1/2}$ when we segment white tissue.

T function is fixed for all pixels in the image which have the same intensity since it has also the same $\Pr(I_{i,j})$. This function will provide us two values, bigger intensity than RA and smaller one. But we only use nearest one of them to RA as the threshold for homogeneity test.

The Algorithm:

Our Method will be as follows:

a. Start our algorithm from the seed(s) pixel(s) which the user select,
b. Add the neighbors of seed pixel to region candidate list and
c. Calculate T_1 and T_2 from Eq.(3) and Eq.(4), substitute them in Eq.(2) for the pixel intensity value which has minimum $f(I_{i,j})$, and if this pixel satisfy Eq.(1) add it to the region and put it as new seed.

The steps (ii) and (iii) will be repeated until the pixel intensity value which has minimum $f(I_{i,j})$ with its threshold dose not satisfy Eq.(1), since all pixels in the region candidate list after this pixel will not also satisfy Eq.(1).

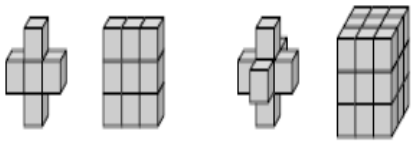

2D neighbors 3D neighbors

Figure 2. Pixel and its neighbors for 2D and 3D

The pixels neighbors in 2D and 3D are 4 or 8 pixels and 6 or 26 pixels respectively as shown in Figure 2. In the next section, we will present the results obtained by our method.

EXPERIMENTAL RESULTS

The experiments were performed with several data sets using MATLAB. We apply the proposed technique to T1-weighted MRI phantom with slice thickness of 1mm, generated at various noise levels and spatial intensity non-uniformity (RF) levels [25]. We generate various inhomogeneities and boundary weakness by controlling noise and RF respectively. We use 4 and 6 neighbors for 2D and 3D respectively. In our algorithm, we set the parameters $\beta_1=\beta_1=3.2$ and $\beta_1=2.2$.

To demonstrate the advantage of the proposed over the others techniques in terms of accuracy, we use average overlap metric (AOM) [24] as a metric to evaluate the performance of image segmentation algorithms. The *AOM* is computed as follows:

$AOM(A, B) = 2|A \cap B| / (|A| + |B|)$,

Where A represents the set of results obtained by the proposed technique and B represents the set of the ground truth data. These metrics reach a value of 1.0 for results that are very similar and is near 0.0 when they share no similarly classified voxels.

Segmentation of Brain MRIs:

We applied our technique to segment MRIs from BrainWeb phantom data [25] generated at various noise levels (0%, 1%, 3%, 5%, 7%, and 9%) and spatial RF levels (0%, 20%, and 40%). We generate various inhomogeneities and boundary weakness by controlling noise and RF respectively. For 2D and 3D we used 4 and 6 pixels neighbors respectively.

Figure 3 shows original slice#62 with noise level 3% and RF level 20% obtained from BrainWeb [25], ground truth of this slice and segmentation results of WM and GM respectively with $\beta_1=\beta_1=3.2$ and $\beta_1=2.2$. Figure 4 shows segmentation results of WM by using the proposed technique using

BrainWeb [25] with noise levels 1% and 9% and RF levels 0%, 20% and 40%.

Figure 5 shows brain MRIs from BrainWeb [25] with RF 20% and noise level 3%, from slice#61 to slice#72, the first row show original slices and second row shows 3D segmentation results. Figure 6 shows the 3D reconstruction of WM and GM segmentation 3D MRIs from BrainWeb [25], the original slices are $181 \times 181 \times 217$ voxels. a) and d) show the ground truth surface of WM and GM respectively, c) and e) show Ayman et al.[3] surface of WM and GM respectively, c) and f) show our method surface of WM and GM respectively.

Segmentation of CT images:

We also applied our technique to segment CT images from DicomWeb [26]. Figure 7 shows 3D CT images from slice#151 to slice#160, the first row shows original slices and second row shows 3D segmentation results. Figure 8 shows the 3D reconstruction surgical repair of facial deformity, the original slices are $512 \times 512 \times 361$ voxels.

Accuracy and Comparison:

Table 1 shows *AOM* of WM using our technique for the BrainWeb data set [25] at various noise and RF levels, these results show that our algorithm is very robust to noise and intensity homogeneities and inhomogeneities. According to Zijdenbos [24] statement that *AOM* > 0.7 indicates excellent agreement; our technique has desired performance in cortical segmentation. The best *AOM* are achieved for low noise and RF levels, for which values of *AOM* higher than 0.97.

Table 2 shows *AOM* of WM using different techniques for the BrainWeb data. In this Table, we compare our method with Ayman et al.[3], Del-Fresno et al.[4] and Yu et al.[7] techniques. In particular, although the segmentation quality logically deteriorates in the presence of noise and variations in intensity, the robustness of the present technique is highly satisfactory even comparing with the results of other segmentation techniques [3, 4, 7].

Table 1. *AOM* for segmentations of WM on simulated T1-weighted MRIs data [25] in different noise and RF levels.

Noise/RF		0		20%		40%
0%		0.97		0.97		0.96
1%		0.97		0.97		0.96
3%		0.96		0.96		0.95
5%		0.95		0.94		0.93
7%		0.93		0.94		0.92
9%		0.92		0.91		0.89

Table 2. *AOM* for WM using the BrainWeb [25].

Noise	3%			9%	
RF	0%	40%		0%	40%
Our method	0.96	0.95		0.92	0.89
Ayman et al.[3]	0.95	0.94		0.91	0.87
Del-Fresno et al.[4]	0.94	0.89		0.91	0.87
Yu et al.[7]	0.90	0.90		0.88	0.88

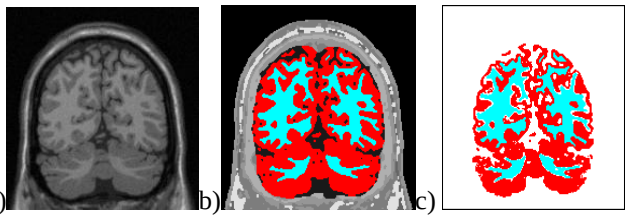

Figure 3. Results for brain MRIs, from BrainWeb [25], a) is original slice#62 with RF 20% and noise level 3%; b) is ground truth, and c) is the segmentation result of WM and GM from a) slice by our technique after using median filtering.

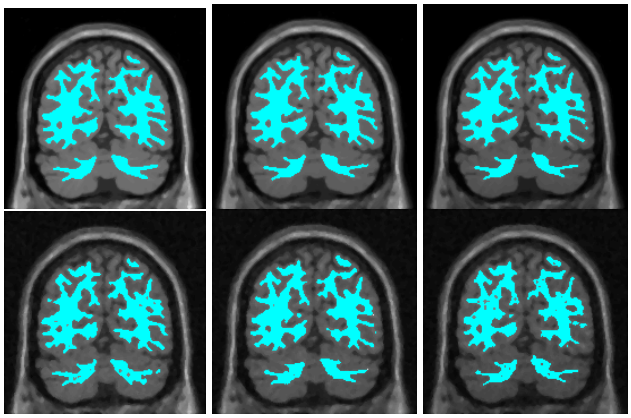

Figure 4. Segmentation of WM from slice#62. Columns 1 to column 3 are RF levels (0%, 20%, and 40%) respectively, row 1 and row 2 are noise levels 1% and 9% respectively.

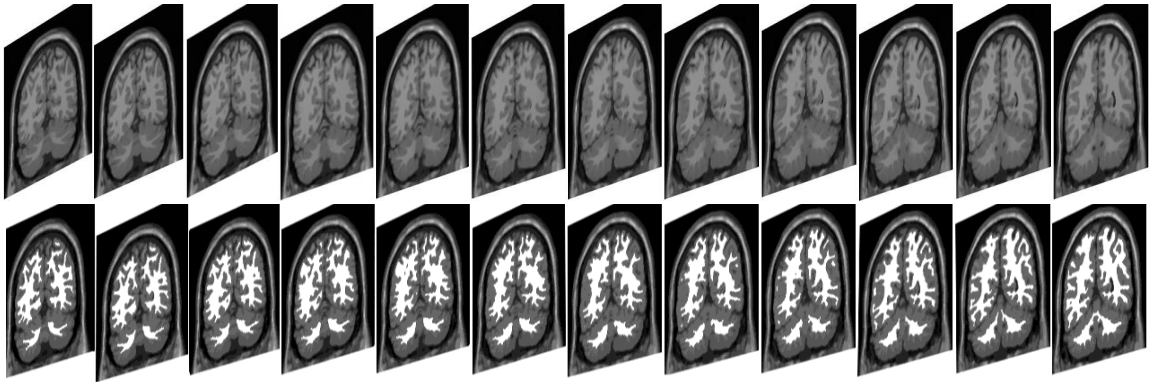

Figure 5. Original slices in first row and 3D Segmentation results of WM in second row, from BrainWeb [25] with RF 20% and noise level 3%, from slice#61 to slice#72.

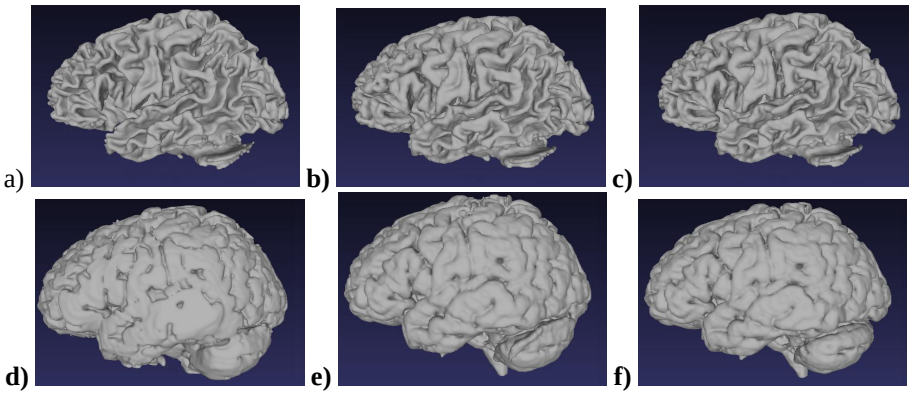

Figure 6. Results for 3D brain MRIs. a) to c) are WM surfaces and d) to f) are GM surfaces of ground truth, Ayman et al.[3] and results obtained by our technique after using median filtering respectively.

CONCLUSIONS

A new RG technique is proposed for segmenting MRIs with noise levels (0%, 1%, 3%, 5%, 7%, and 9%) and RF levels (0%, 20%, and 40%) and CT images which contain weak boundaries by proposing an automatic threshold. The proposed method has several advantages compared with previous segmentation strategies. One of the most important improvements is generating an automatic threshold for different volumes. We used a few seeds to identify the regions. Furthermore, we used the probability of pixels intensities of MRIs and CT images to extract tissue(s) in 2D and 3D images.

The growing process incorporates information of the local neighborhood and global probability of pixels intensities of each voxel in the region.

The technique was tested on the segmentation of complex 18 anatomical 3D structures from a standard synthetic phantom, and one CT scans. These test images showed that segmentation results are much closed to ground truth, the segmentation of white matter show excellent performances, the average exceeding 94%. We will be able to segment real images which have noise levels from 0% to 9% and RF levels from 0% to 40%.

REFERENCES

[1] M. Forouzanfar, N. Forghani, and M. Teshnehlab, Parameter optimization of improved fuzzy c-means clustering algorithm for brain MR image segmentation, Engineering Applications of Artificial Intelligence, 23, 2010, 160–168.

[2] O. Gloger, J. Kühn, A. Stanski, H. Völzke, and R. Puls, A fully automatic three-step liver segmentation method on LDA-based probability maps for multiple contrast MR images, Magnetic Resonance Imaging, 28, 2010, 882–897.

[3] A. Ayman, , T. Funatomi, M. Minoh, Z. Elnomery, T. Okada, K Togashi, T. Sakai and S. Yamada, New Region Growing Segmentation Technique for MR Images with Weak Boundaries, IEICE conference MI2010-79, JAPAN, 2010, 71-76.

[4] M. Del-Fresno, M. Vénere, and A. Clausse, A combined region growing and deformable model method for extraction of closed surfaces in 3D CT and MRI scans, Computerized Medical Imaging and Graphics, 33, 2009, 369–376.

[5] L. Wang, L. Chunming, S. Quansen, X. Deshen, and K. Chiu-Yen, Brain MR image segmentation using local and global intensity fitting active contours/surfaces, MICCAI 2008, Part I, LNCS 5241, 2008, 384–392.

[6] Y. -T. Wu, F. Y. Shih, J. Shi, and Wu Yi.-T., A top-down region dividing approach for image segmentation, Pattern Recognition, 41, 2008, 1948 – 1960.

[7] Z. Q. Yu, Y. Zhu, J. Yang, Y. M. Zhu, A hybrid region-boundary model for cerebral cortical segmentation in MRI, Computerized Medical Imaging and Graphics, 30, 2006, 197–208.

[8] Y. Boykov, and V. Kolmogorov, An experimental comparison of min-cut/max- flow algorithms for energy minimization in vision. IEEE Transactions on Pattern Analysis and Machine Intelligence, 26(9), 2004, 1124–1137.

[9] K. Belloulata, and J. Konrad, Fractal image compression with region-based functionality, IEEE Trans. Image Process, 11(4), 2002, 351–362.

[10] Y. Chen, and J. Z. Wang, A region-based fuzzy feature matching approach to content-based image retrieval, IEEE Trans, Pattern Anal. Machine Intell., 24(9), 2002, 1252–1267.

[11] O. J. Tobias, and R. Seara, Image segmentation by histogram thresholding using fuzzy sets, IEEE Trans. Image Process, 11(12), 2002, 1457–1465.

[12] L. Vese, and T. Chan, A multiphase level set framework for image segmentation using the Mumford and Shah model. Int'l. J. Comp., 50, 2002, 271–293.

[13] Y. Boykov, and M. -P. Jolly, Interactive graph cuts for optimal boundary and region segmentation of objects in n-d images. In Proc. ICCV, 1, 2001, 105–112.

[14] T. Chan, and L. Vese, Active contours without edges. IEEE Trans. Imag. Proc., 10, 2001, 266–277.

[15] C. Baillard, P. Hellier, and C. Barillot, Segmentation of brain 3D MR images using level sets and dense registration, Medical Image Analysis, 5, 2001, 185–194.

[16] Y. Boykov, and M. -P. Jolly, Interactive organ segmentation using graph cuts. In Proc. MICCAI, 2000, 276-286.

[17] H. Tang, E. X. Wu, Q. Y. Ma, D. Gallagher, G. M. Perera, and T. Zhuang, MRI brain image segmentation by multi-resolution edge detection and region selection, Computerized Medical Imaging and Graphics, 24, 2000, 349–357.

[18] K. Haris, S. N. Efstratiadis, N. Maglaveras, and A. K. Katsaggelos, Hybrid image segmentation using watersheds and fast region merging, IEEE Trans. Image Process, 7(12), 1998, 1684–1699.

[19] S. A. Hojjatoleslami, and J. Kittler, Region growing: a new approach, IEEE Transactions on Image Processing, 7, 1998, 1079–1084.

[20] A. Mehnert, and P. Jackway, An improved seeded region growing algorithm, Pattern Recognition Letters, 18, 1997, 1065–1071.

[21] S. C. Zhu, and A. Yuille, Region competition: unifying snakes, region growing, and Bayes/MDL for multiband image segmentation, IEEE Trans. Pattern Anal. Machine Intell., 18(9), 1996, 884–900.

[22] R. Adams, and L. Bischof, Seeded region growing, IEEE Transactions on Pattern Analysis and Machine Intelligence, 16, 1994, 641–647.

[23] Y. L. Chang, and X. Li, Adaptive image region growing, IEEE Transactions on Image Processing, 3, 1994, 868–873.

[24] A. P. Zijdenbos, MRI segmentation and the quantification of white matter lesions, PhD thesis, Vanderbilt University, Electrical Engineering Department, Nashville, Tennessee; December 1994.

[25] http://www.bic.mni.mcgill.ca/brainweb/

[26] http://pubimage.hcuge.ch:8080/

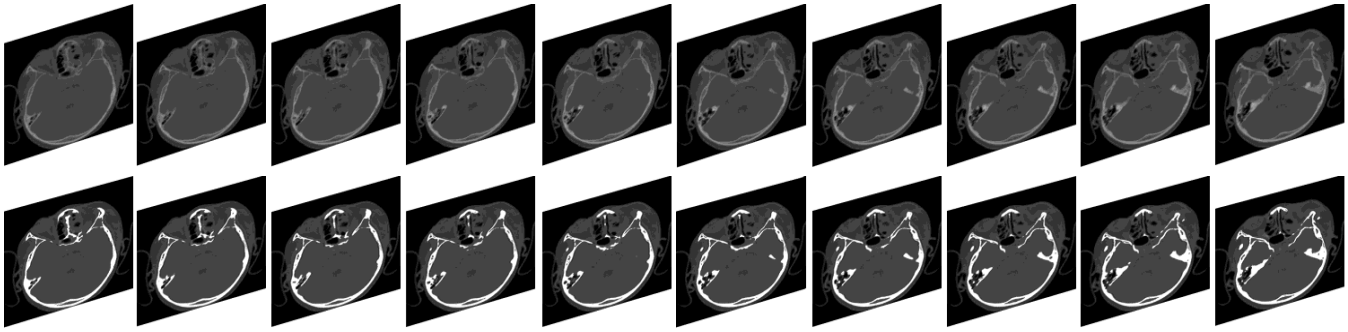

Figure 7. Original slices in first row and 3D Segmentation results of skull CT in second row, from DicomWeb [26], from slice#151 to slice#160.

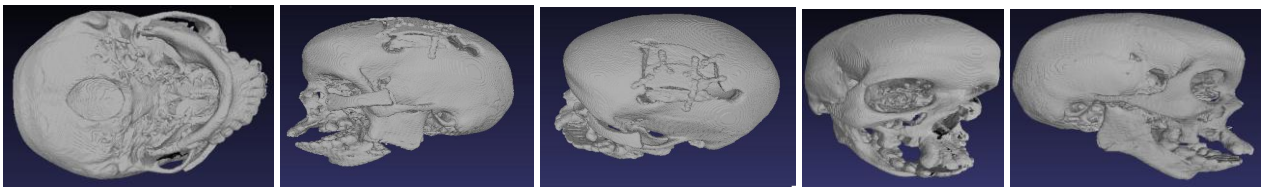

Figure 8. 3D reconstruction of skull CT volume from DicomWeb [26], in different views obtained by our me thod.